


Experimental study on the performance of a highly efficient NE-1 absorbent for CO₂ capture


Chenzhi Huang , **Yongda Cao** and **Yaxin Li**, Research Institute of Natural Gas Technology, PetroChina Southwest Oil & Gasfield Company, Chengdu, Sichuan, China

Qi Li, PetroChina Southwest Oil & Gasfield Company, Chengdu, Sichuan, China

Qiang Liu, New Energy Division, PetroChina Southwest Oil & Gasfield Company, Chengdu, Sichuan, China

Lin Xia, Natural Gas Purification Plant General, PetroChina Southwest Oil & Gasfield Company, Chongqing, China

Xiujun Peng, Research Institute of Natural Gas Technology, PetroChina Southwest Oil & Gasfield Company, Chengdu, Sichuan, China

Hairong Yue , School of Chemical Engineering, Sichuan University, Chengdu, Sichuan, China

Abstract: CO₂ capture by absorption and stripping with aqueous amine is a well-understood and widely used technology. However, drawbacks still exist in the practical applications, such as high energy consumption and easy degradation of the absorbents during the desorption process. In this paper, a novel NE-1 absorbent was developed, and its suitable operating conditions were determined: concentration (45 wt. %), absorption temperature (40 °C), and desorption temperature (100 °C). The NE-1 absorbent exhibits a high CO₂ absorption capacity of 3.73 mol/kg, 1.33 times that of 30% monoethanolamine (MEA). After optimizing with carbamide as a corrosion inhibitor, 45% NE-1a1 may attain an effective CO₂ capacity of 2.5 mol/kg and over 70% desorption rate in five cycles, demonstrating excellent cycling stability performance. The research results have significant implications for developing an efficient and stable commercial carbon capture solvent and promoting the development of carbon reduction technologies. © 2024 Society of Chemical Industry and John Wiley & Sons, Ltd.

Keywords: CO₂ capture; liquid amine; absorption; corrosion inhibitor; thermal degradation

Introduction

With the increase in population and rapid economic growth, the consumption of primarily fossil fuel-based non-renewable energy continues to rise,¹ resulting in significant carbon dioxide (CO₂) emissions and adverse impacts

on global climate and the environment.² According to the International Energy Agency's (IEA) "2022 CO₂ Emissions" report, global CO₂ emissions from energy combustion and industrial processes reached approximately 36.8 billion tons in 2022, reaching a new historical high.³ China's total CO₂ emissions exceed 10 billion tons per year, accounting for nearly 30% of the

Correspondence to: Chenzhi Huang, Research Institute of Natural Gas Technology, PetroChina Southwest Oil & Gasfield Company, Chengdu, Sichuan 610213, China. E-mail: huang_chzh@petrochina.com.cn

Received December 14, 2023; revised March 4, 2024; accepted March 14, 2024

Published online at Wiley Online Library (wileyonlinelibrary.com). DOI: 10.1002/ghg.2272

global total.⁴ Carbon capture, utilization, and storage (CCUS) technology represents one of the typical carbon emission reduction technologies due to its technological maturity and economic viability.⁵ Carbon capture is an important pathway for reducing CO₂ emissions and serves as a primary step in the resource utilization of CO₂. The development of advanced carbon capture technologies has become a research focus in the field of carbon emission reduction.

Amine absorption is currently the most widely used industrial carbon capture technology, which utilizes the chemical reaction between amine molecules and CO₂ to separate CO₂ from the feed gas. The CO₂ is then released by reversing the reaction through heating, allowing for the separation of CO₂ from the solvent and enabling the regeneration of the capture solution for recycling. Aqueous amine solutions are the main absorbents used in industrial applications. However, these solutions have a high specific heat capacity, enthalpy and heat of vaporization, and require high regeneration temperatures (120–150 °C).⁶ In the desorption process, the enthalpy and heat of vaporization of the solvent account for approximately 70% of the total energy consumption in the capture process,^{7,8} resulting in high energy consumption and low capture efficiency for aqueous amine solutions.⁹

It is worth mentioning that industrial CO₂ absorbents require good stability and should not undergo thermal decomposition under high-temperature regeneration conditions (typically above 100 °C). At the same time, they should minimize their corrosiveness to equipment. Currently, typical industrial amine absorbents incorporate corrosion inhibitors (such as imidazoline quaternary ammonium salts) during operation to reduce the corrosiveness of amine absorbents to equipment.^{10,11} However, the addition of corrosion inhibitors can affect the absorption performance and stability of CO₂ absorbents to some extent. Therefore, the stability of the absorbent is crucial for its industrial application.

In summary, energy consumption and stability are the main factors currently limiting the industrial application of absorption-based CO₂ capture technologies. The development of advanced absorption-based CO₂ capture technologies relies on the development of highly efficient and stable carbon capture solvents. Therefore, it is of utmost importance

to develop new capture solvents based on existing absorption-based carbon capture processes to improve process stability and further reduce energy consumption. Current research on CO₂ absorption solvents mainly focuses on high absorption capacity, low specific heat capacity, and low saturation vapor pressure, often overlooking practical application indicators such as physical properties and cost. For example, ionic liquid-based CO₂ absorbents have a high CO₂ absorption capacity, but their high cost and viscosity hinder their industrial application.^{12,13} Phase-change absorbents automatically separate the CO₂-rich phase from the lean phase after CO₂ absorption, reducing the energy consumption of rich solution regeneration.^{14,15} However, available phase-change absorbent reactors are expensive, and the high CO₂ concentration in the rich phase generally leads to high viscosity, which is unfavorable for desorption.¹⁶ By adding organic alcohol solvents such as glycerol, propylene glycol, ethylene glycol, and polyethylene glycol, amine desorption reactions can be performed at lower temperatures (80–100 °C), reducing desorption energy consumption. Additionally, the polar hydroxyl groups in the solvent can enhance CO₂ absorption rates, thereby improving CO₂ capture capacity. However, currently reported organic solvents such as methanol, ethylene glycol (with a saturated vapor pressure of 133 Pa at 20 °C), and propylene glycol (with a viscosity of 330 mPa s at 40 °C) have disadvantages such as high vapor pressure, toxicity, and high viscosity, making them unsuitable for industrial operations.^{17–19}

Based on this, this paper developed a new NE-1 amine solution for CO₂ absorption, which has appropriate viscosity and heat capacity. Combined with the existing absorption desorption process, the suitable NE-1 concentration (45 wt.%), absorption temperature (40 °C) and desorption temperature (100 °C) were selected, and the CO₂ absorption capacity and absorption/desorption performance were determined. In addition, the amine solvent system has good stability, and its composition has not changed significantly after 50 hr thermal degradation test after adding corrosion inhibitor. The CO₂ absorption capacity is still as high as 3.73 mol/kg, increasing 33% compared to the 30wt% MEA commercial benchmark absorption system, which has obvious industrial application prospects.

Materials and method

Chemicals and instrument

NE-1 solvent was developed by the natural gas Research Institute of PetroChina Southwest Oil & Gas field Company. Ethanolamine (MEA), carboamide, methionine, and malondiamine acetic acid were analytically pure and purchased from Chengdu Cologne Reagent Co., Ltd. CO₂/N₂ mixture, high-purity N₂ and other gases were purchased from Air Liquide Co., Ltd.

Mass flowmeter (MFC, Beijing Qixing Huachuang flowmeter Co., Ltd.); CO₂ infrared analyzer (FN316B, Shaanxi feiente Instrument Technology Co., Ltd.); thermogravimetric analyzer (Netzsch STA 449F5); differential scanning calorimetry analyzer (Netzsch DSC 214); working glass float gauge (JJG42-2011); rotary viscometer (ndj-8s, Shanghai Hengping instrument factory); closed flash point tester (SYD-261-1); gas chromatography-mass spectrometry (GCMS-QP2010 plus, Shimadzu, Japan).

Measurement of CO₂ loading

The CO₂ loading measurement is carried out by acid titration method. Figure 1 shows the titration device. All connections in the device are connected with transparent silicone tubes. The measuring tube is equipped with a red indicator of acid for easy reading.

The experimental process is as follows: use the pipette gun to measure 100 µL put the sample to be tested into a 50 mL grinded conical flask and weigh it, and record the sample mass as *M*. Connect the conical flask with the glass bronchus and keep the interface airtight. Close the valve of the measuring pipe to make the whole device form a closed system, and record the initial reading *V*₀ of the measuring pipe. Add 2 mL of dilute hydrochloric acid (1 mol/L) to the grinded conical flask through an acid burette to ensure that the acid is excessive, and the acid addition volume is recorded as *V*₁. A large amount of CO₂ gas is rapidly released when the sample is in contact with the acid. Shake the conical flask vigorously so that CO₂ can be completely desorbed. When the liquid level of the indicator is stable, adjust the height of the liquid level pipe connected with the atmosphere to make it level with the indicator page in the measuring pipe, and record the liquid level reading of the measuring pipe, which is *V*₂. After titration, open the polytetrafluoroethylene valve above the measuring pipe to release gas and restore the system to its original state.

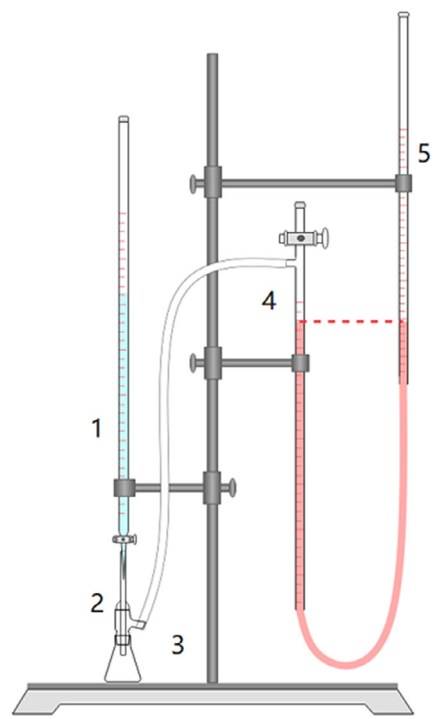


Figure 1. CO₂ titration device (a: acid burette, b: glass bronchus, c: 50 mL grinded conical flask, d: measuring tube with polytetrafluoroethylene valve, e: liquid level tube connected to the atmosphere).

The following formula is used to calculate the CO₂ load. For the CO₂ volume at room temperature and room pressure, the ideal gas state equation is used for simple correction. The calculation formula of CO₂ load is as follows^{3,20}:

$$C_{\text{CO}_2} = \frac{(V_2 - V_1 - V_0)}{22.4} \times \frac{273.15}{T + 273.15} \times \frac{P}{101.325} \div M \quad (1)$$

*C*_{CO₂} is the load of CO₂ per unit mass of sample, mol/kg; The unit of *V*₀ *V*₁ *V*₂ is mL; *T* is the room temperature during titration, °C; *P* is pressure, kPa; *M* is the mass of the sample, g. Each sample was titrated three times in parallel, and the mean value was taken. The titration error was about ± 0.05 mol/kg.

Measurements of reactions heat

The reaction heat was measured by thermogravimetric analyzer with 10 mg sample, the heating rate was set to 2 K/min, and the purge gas CO₂ and protective gas N₂

flow rates were 30 and 20 mL/min, respectively. The absorption temperature was 40 °C.

$$\Delta n = \frac{Y_2 - Y_1}{44.01} \quad (2)$$

$$\Delta H = \frac{\Delta H^*}{\Delta n} \quad (3)$$

Where Δn is the absorption capacity of CO₂ per unit weight of NE-1, unit is mol_{CO2}/g, Y_2 and Y_1 are the mass ratio of absorbent after absorption and before absorption (%), and ΔH^* is the integral area of heat flow (J/g_{CO2}).

Tests of specific heat capacity

The specific heat capacity was measured by differential scanning calorimetry (DSC). Heat the system temperature from 298 to 373 K with a heating rate of 10 K/min and maintain the temperature for 10 min at the starting and ending temperatures, respectively.

$$C_p = \frac{60(A_S - A_B)}{m_s \beta} \quad (4)$$

C_p is the specific heat of absorbent. A_S and A_B are the heat flow of sample test and blank test respectively, m_s is the mass of test sample, and β is the heating rate.

Density and viscosity tests

Solvent density was measured by working glass float meter (JJG42-2011); The viscosity was measured by a rotary viscometer (NDJ-8S, Shanghai Hengping instrument factory), with an error of $\pm 2\%$.

Equilibrium solubility tests

In the equilibrium solubility experiment, the partial pressure of water (P_{H_2O}) is approximately calculated by Raoult's Law:

$$P_{H_2O} = \gamma_{H_2O} \times P_{H_2O}^{vap} \quad (5)$$

Where, γ_{H_2O} is the molar ratio of water in solution, $P_{H_2O}^{vap}$ is the saturated vapor pressure of H₂O, kPa, which was approximate estimation by Antoine equation as follows:

$$\lg P_{H_2O}^{vap} = 7.07406 - \frac{1657.46}{T + 227.02} \quad (6)$$

The partial pressure of carbon dioxide ($P_{CO_2}^*$) of the system during desorption process was calculated as formula 7:

$$P_{CO_2}^* = \gamma_{CO_2} \times (101.325 - P_{H_2O}) \quad (7)$$

Where, γ_{CO_2} is the CO₂ concentration of inlet, set to 1%, 5%, 10%, 15%, 20%, 30%, and 100%, respectively.

The ratio of CO₂ partial pressure to H₂O partial pressure is:

$$\alpha = P_{CO_2}^* / P_{H_2O} \quad (8)$$

The Henry constant was calculation using following equation:

$$P_{CO_2}^* = K_{b,CO_2} b_{CO_2} \quad (9)$$

Where, $P_{CO_2}^*$ is the calibrated CO₂ partial pressure, kPa, K_{b,CO_2} is the Henry constant, kPa·kg/mol, b_{CO_2} is the mass molar concentration of CO₂ in the solution after absorption saturation, mol/kg.

Tests of CO₂ absorption/desorption performance

The schematic diagram of the CO₂ absorption/desorption device is shown in Fig. 2. In the CO₂ absorption experiment, the flow rate of CO₂ and N₂ is adjusted by mass flowmeter to form a 15 ± 0.05 vol% CO₂ mixture gas (500 mL/min) to simulate flue gas. Before the experiment, the whole system was purged with N₂, and the gas was bubbled into a three-port flask to react with 50 mL absorbent. The temperature of the absorption process was controlled by a water bath, and magnetic stirring was maintained to enhance gas-liquid mass transfer. After condensation and sulfuric acid drying, the outlet gas enters the CO₂ infrared analyzer for online monitoring of CO₂ concentration. When the outlet concentration reaches 15 ± 0.1 vol% and remains unchanged for 10 min, it is regarded as absorption saturation.

The process of CO₂ desorption used N₂ (200 mL/min) as the purge gas, and the desorption temperature was controlled through an oil bath. It is believed that CO₂ desorption is finished when the concentration of CO₂ in the outlet gas is less than 0.15 vol%.

The CO₂ absorption rate (r_{abs}) and desorption rate (r_{des}) of the absorbent were calculated according to the following equation²¹:

$$r_{abs} = V_{m,gas} \frac{G_{N_2}}{V} \left(\frac{\varphi_0}{1 - \varphi_0} - \frac{\varphi_1}{1 - \varphi_1} \right) \quad (10)$$

$$r_{des} = V_{m,gas} \frac{G_{N_2}}{V} \left(\frac{\varphi_1}{1 - \varphi_1} \right) \quad (11)$$

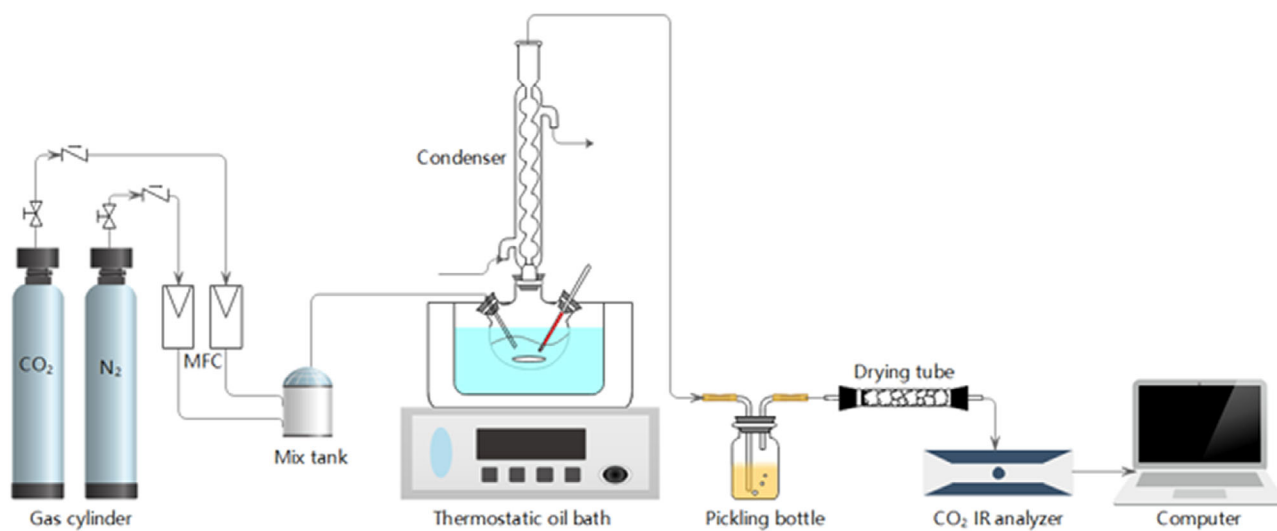


Figure 2. Absorption/desorption experimental device.

Due to the low solubility of the absorbent for N_2 , it can be assumed that the volume of N_2 does not change during absorption and desorption and therefore can be used as an internal standard gas. Where, V is the volume of absorption solution, mL; φ_0 and φ_1 respectively represents the volume fraction of CO_2 in the inlet and outlet of the reaction device; G_{N_2} represents the volume flow of N_2 under standard conditions, mL/min; and $V_{m, gas}$ are ideal gas molar volumes, 22.4 L/mol.

The absorption capacity (F_{abs}) and desorption capacity (F_{des}), mmol/L, were calculated by integrating the absorption rate and desorption rate over time (t):

$$F_{abs} = \int_0^t r_{abs} dt \quad (12)$$

$$F_{des} = \int_0^t r_{des} dt \quad (13)$$

Study on stability of absorbent

In the cyclic stability experiment, the volume of 45% NE-1 is 150 mL, the flow rate of CO_2 mixture is 700 mL/min, and the flow rate of desorption N_2 is 200 mL/min. The criterion for determining absorption saturation was still that the outlet CO_2 concentration reaches 15 ± 0.1 vol% and the judgement for desorption completion was that the outlet CO_2 concentration is below 0.25 vol%.

Further investigation was conducted on the effects of three corrosion inhibitors on the NE-1 cyclic

absorption performance, with a dosage of 1 wt.%. The 45% NE-1 sample with added carbamide, methionine, and malondiamine acetic acid were labeled as NE-1a1, NE-1b1, and NE-1c1, respectively. The absorption experiment was carried out at 40 °C, and the desorption experiment was carried out at 100 °C. 30% MEA was used as the control sample.

The thermal stability of absorption solutions has also been studied. Put 50 mL of 45% NE-1, NE-1a1, NE-1b1, and NE-1c1 solvents that have absorbed CO_2 into autoclave (with CO_2 loading controlled at 0.5–0.6 mol/L) and replace the residual oxygen in the autoclave with N_2 . Keep the autoclave at 120 °C for 50 hr and analyze the pyrolysis products by gas chromatography-mass spectrometry (GC-MS).

Results and discussion

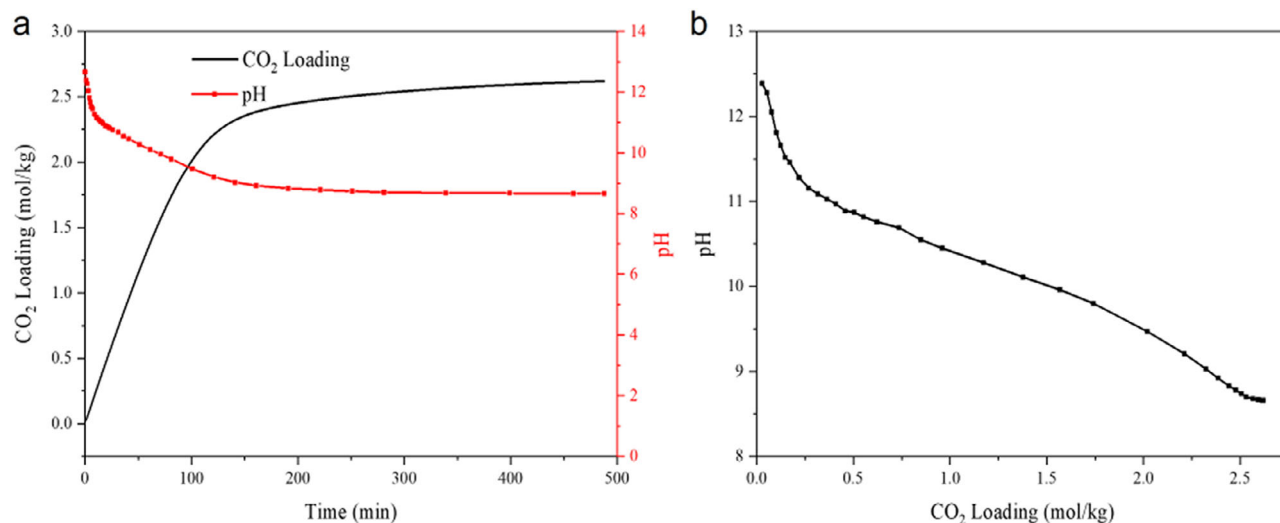
Physical properties of NE-1

The physical properties of pure NE-1 are shown in Table 1, with a high viscosity at room temperature, reaching 32.39 mPa·s. After diluting NE-1 concentration to 45 wt.% with ultrapure water, the viscosity significantly decreased to 6.03 mPa·s at 30 °C. Appropriate solvent viscosity can lower pump transportation power consumption and help with CO_2 mass transfer in the liquid phase. The viscosity of the absorbing solvent decreases as the temperature rises; while, temperature or NE-1 concentration has little effect on density.

Figure 3 shows the pH curve of 45% NE-1 solution as a function of CO_2 loading. The pH value of 45% NE-1

Table 1. Physical parameters of pure NE-1 and 45% NE-1 solution.

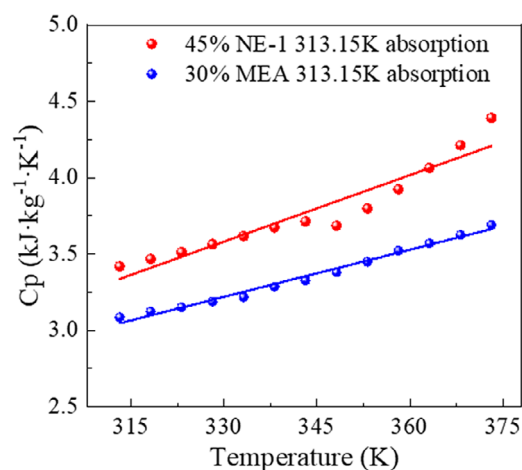
| Sample | Temperature | Density/ g·mL ⁻¹ | Viscosity/ mPa·s |
|----------|-------------|--------------------------------|---------------------|
| NE-1 | 25 °C | 0.987 | 32.4 |
| 45% NE-1 | 30 °C | 1.013 | 6.03 |
| 45% NE-1 | 40 °C | 1.007 | 4.11 |
| 45% NE-1 | 80 °C | 0.976 | 1.21 |

**Figure 3.** 45% NE-1 (a) CO₂ loading and pH change with time; (b) pH versus load curve.

lean solution is about 12.7, and after CO₂ absorption saturation (3.5 mol/kg), the pH value drops to 8.65. After absorbing CO₂, the viscosity of 45% NE-1 increased from 6.03 to 10.7 mPa·s, which is due to the formation of carbamate.

The specific heat capacity of the absorbent and the reaction heat of CO₂ absorption are significant factors influencing the energy consumption for CO₂ capture. The specific heat capacity test results of 45% NE-1 after CO₂ absorption saturation are shown in Fig. 4. There is a linear relationship between volumetric specific heat and temperature of NE-1 and MEA systems. Overall, the specific heat of the NE-1 system is higher than that of MEA at the same temperature, and the increase rate of NE-1 specific heat with temperature is faster. At 363.15 K, the specific heats of 45% NE-1 and 30% MEA solutions saturated with CO₂ are 4.07 and 3.59 kJ·kg⁻¹·K⁻¹, respectively. This indicates that MEA absorbent has more advantages in reducing regeneration sensible heat compared to NE-1.

The CO₂ absorption reaction heat of 30% MEA solution was determined to be 81.66 kJ/mol_{CO2} via TG experimental analysis. This value is consistent with the

**Figure 4.** The specific heat and temperature curve of 45% NE-1 and 30% MEA rich solution.

data published in the literature, indicating that this method of determining the reaction heat is reliable. The reaction heat of 45% NE-1 obtained is 74.26 kJ/mol_{CO2}, which is lower than that of the 30% MEA system (Table 2).

Table 2. Thermodynamics parameters of 45% NE-1 and 30% MEA.

| Thermodynamics parameters | 45% NE-1 | 30% MEA |
|--|----------|---------|
| $\Delta H_{\text{reac}}(\text{kJ/mol}_{\text{CO}_2})^{\text{a}}$ | 74.26 | 81.66 |
| $C_p(\text{kJ}\cdot\text{kg}^{-1}\cdot\text{K}^{-1})^{\text{b}}$ | 4.07 | 3.59 |

^a Reaction heat of lean solution at 313.15 K.
^b CO₂ saturated solution at 363.15 K.

CO₂ absorption performance of NE-1

The CO₂ absorption performance of NE-1 solutions with different concentrations (35%, 40%, and 45%) and absorption temperatures (30, 40, and 50 °C) were investigated. The CO₂ absorption rate and absorption capacity of NE-1 under different conditions are presented in Figs 5 and 6. The concentration of NE-1 absorbent is the key factor affecting the CO₂ absorption performance.

At the same temperature, the higher the concentration of NE-1 was, the higher the saturation absorption loading and the longer the time required to reach absorption saturation (Fig. 5c, f, and i). Both the absorption temperature and the NE-1 concentration affect the CO₂ absorption rate. At a low absorption temperature, the negative effect caused by the rising solution viscosity on CO₂ absorption rate is stronger than the promoting effect of the increase of NE-1 concentration on mass transfer. This resulted in a faster CO₂ absorption rate of 40% NE-1 solution than 45% NE-1 at 30 °C (Fig. 5a, b). However, at high absorption temperatures, the viscosity of the absorption system decreases, and the enhancement of the absorption kinetics due to an increase in NE-1 concentration dominates, resulting in a 45% NE-1 solution exhibiting the highest CO₂ absorption rate at 50 °C. (Fig. 5g, h).

At the same NE-1 concentration, the CO₂ loading capacity of the system is the highest at 30 °C, and the CO₂ loading gradually decreases as the absorption temperature rises (Fig. 6c, f, and i). This is due to the exothermic character of the absorption process and because CO₂ desorption is more facilitated by high temperatures. According to the Arrhenius formula, the reaction rate constant is proportional to the temperature, so the initial absorption rate is accelerated when the temperature increases. With the progress of the absorption, the CO₂ content in the system

Table 3. CO₂ absorption performance of NE-1.

| Concentration of NE-1 | Absorption temperature/°C | Saturation time/min | CO ₂ loading/mol·kg ⁻¹ |
|-----------------------|---------------------------|---------------------|--|
| 35% | 30 | 233 | 3.23 |
| | 40 | 130 | 3.10 |
| | 50 | 90 | 2.99 |
| 40% | 30 | 235 | 3.45 |
| | 40 | 134 | 3.22 |
| | 50 | 119 | 3.06 |
| 45% | 30 | 262 | 3.61 |
| | 40 | 136 | 3.51 |
| | 50 | 119 | 3.49 |

decreases, and the reaction equilibrium shifts towards CO₂ desorption at high temperatures, resulting in a decrease in the absorption rate of end stage (Fig. 6b, e and h).

The saturated absorption time and saturated absorption capacity of the absorbent under the conditions of different NE-1 concentrations and absorption temperatures are shown in Table 3. When CO₂ absorption is carried out at 50 °C, 35% NE-1 has the shortest saturation time (90 min), but the CO₂ capacity is the smallest (2.99 mol/kg). However, 45% NE-1 exhibits the highest absorption capacity (3.61 mol/kg) when absorbing CO₂ at 30 °C but requires the longest equilibrium time (262 min). Comprehensive analysis shows that selecting a 45% NE-1 solution to absorb CO₂ at 40 °C can achieve both a fast absorption rate (reaching saturation within 136 minutes) and a high saturated absorption capacity (3.51 mol/kg).

Desorption performance of NE-1

After determining the optimal absorption conditions for NE-1, we further investigated the influence of temperature on the desorption performance of NE-1. The desorption rate and desorption amount of 45% NE-1 solution (saturated with CO₂ at 40 °C) were measured under nitrogen flow rate of 200 mL/min under desorption systems at 80, 90, and 100 °C, respectively. As shown in Fig. 7, the desorption rate of CO₂ decreased with the increase of desorption amount, and the decreasing rate gradually slowed down. According to Le Chatelier's principle, with the increase of desorption amount, the CO₂ loading in NE-1

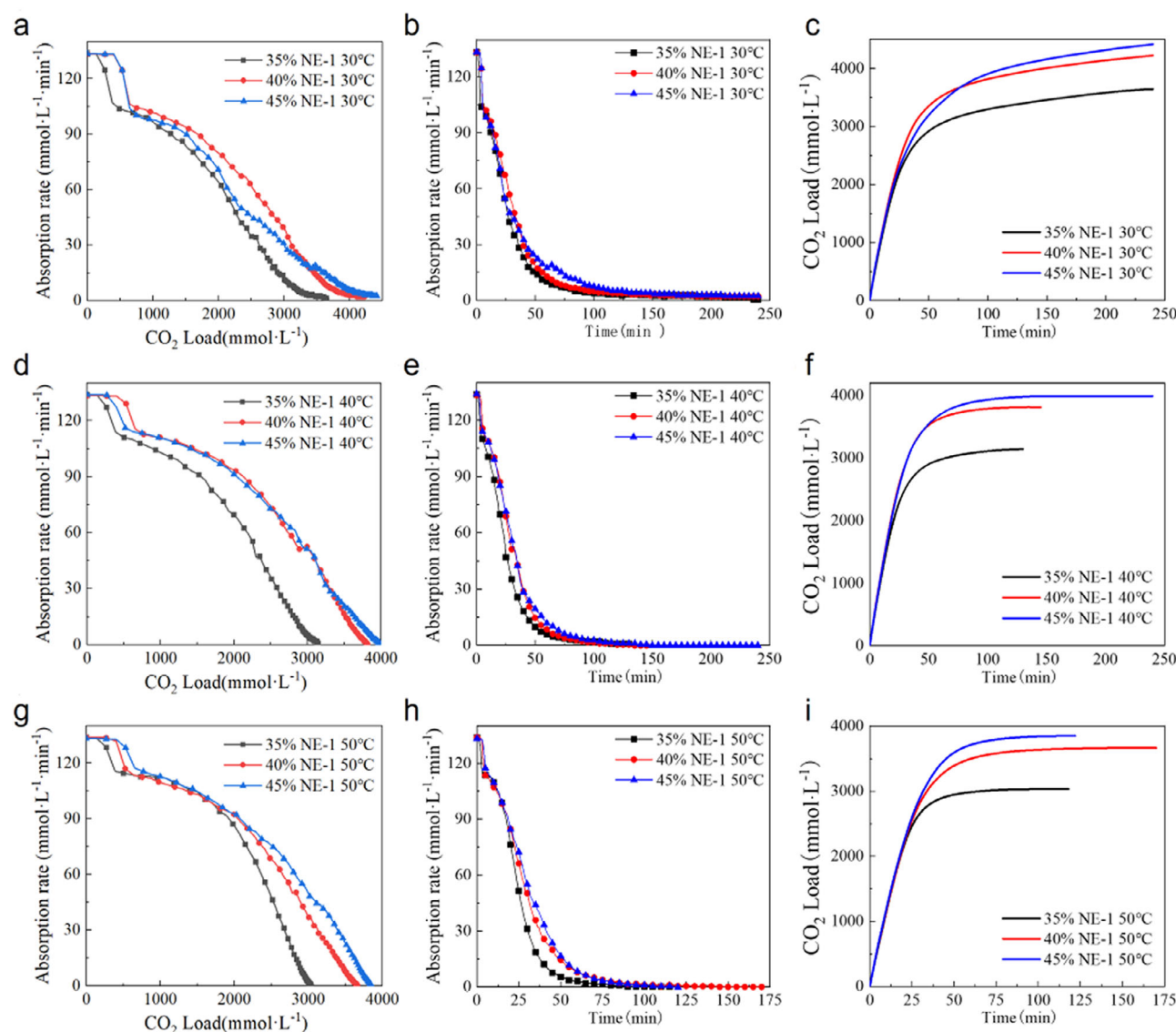


Figure 5. Effect of concentration on absorption performance of NE-1: (a), (d), and (g) are absorption rate-CO₂ loading diagram; (b), (e), and (h) are CO₂ absorption rate-time diagram; and (c), (f), and (i) are CO₂ loading-time diagram.

solution decreases, which makes the desorption rate decrease, and the desorption rate is close to zero, and the system tends to desorption equilibrium.

With the increase of desorption temperature, the initial desorption rate increases, which is due to the endothermic process of desorption reaction, and higher temperature is more conducive to the forward reaction. Meanwhile, the higher the temperature, the more complete regeneration of the absorbent can be achieved in a shorter time. Therefore, the system maintained a high desorption rate during the whole reaction at 100 °C.

Comparison of CO₂ equilibrium solubility between NE-1 and MEA

CO₂ equilibrium solubility is one of the important evaluation factors in the field of energy consumption calculation and industrial process design optimization. We measured the equilibrium solubility of CO₂ in 45% NE-1 at different temperatures (40, 80, and 100 °C) and compared it with commercial MEA absorbents (30%). The results showed that the CO₂ equilibrium solubility of NE-1 system was similar to that of MEA system. At the absorption temperature of 40 °C, the CO₂ loading of 30% MEA is slightly higher than that of 45% NE-1

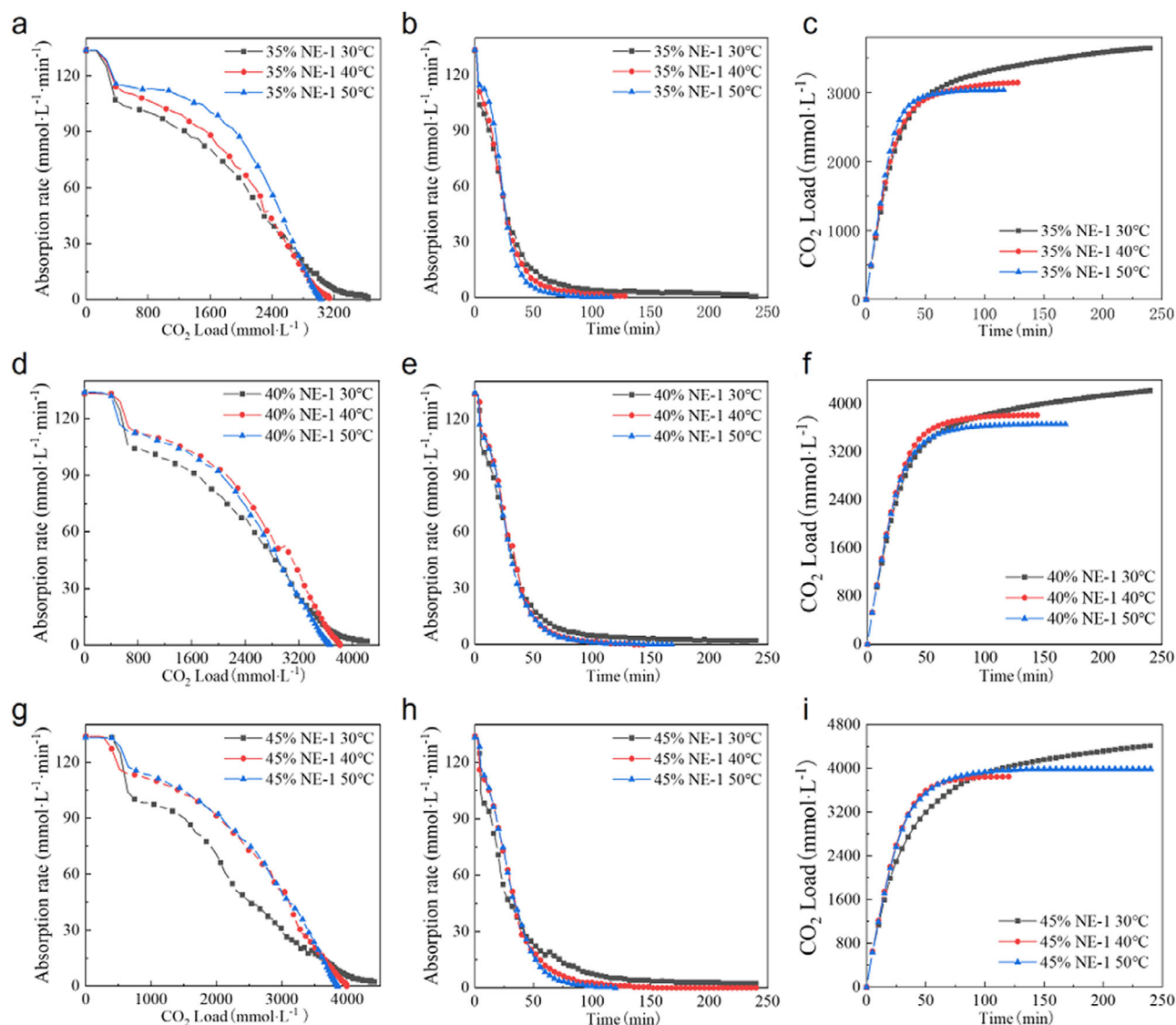


Figure 6. Effect of temperature on absorption performance of NE-1: (a), (d), and (g) are absorption rate- CO_2 loading diagram; (b), (e), and (h) are CO_2 absorption rate-time diagram; and (c), (f), and (i) are CO_2 loading-time diagram.

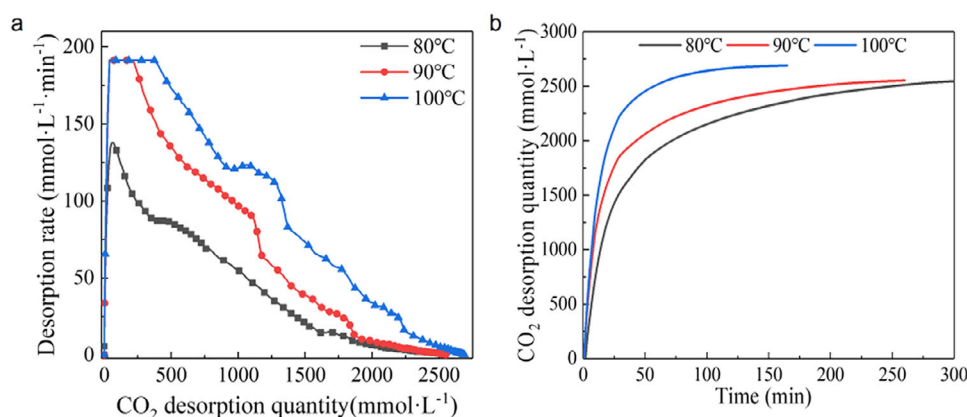


Figure 7. Desorption properties of NE-1 at different temperatures. (a) desorption rate- CO_2 desorption quantity diagram; (b) CO_2 desorption quantity-time diagram.

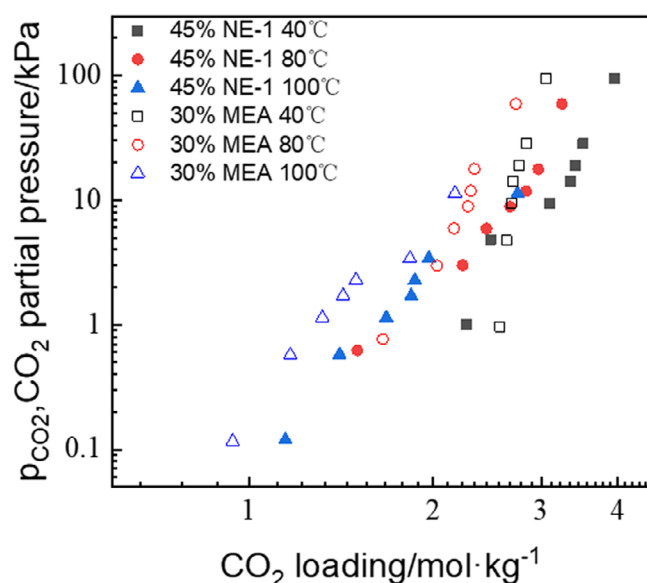


Figure 8. CO₂ equilibrium solubility diagram of 45% NE-1 and 30% MEA.

when the CO₂ concentration is lower than 5%. When the CO₂ concentration increases to 10%, the CO₂ loading of 45% NE-1 is both higher than that of 30% MEA at 40 and 80°C, which indicates that the NE-1 decarbonization agent has certain absorption capacity advantages compared with MEA in absorbing CO₂ from high-concentration flue gas, especially when the CO₂ concentration is over 30% (Fig. 8).

Performance of NE-1 with added corrosion inhibitors

In industry, corrosion inhibitors are widely employed to alleviate equipment corrosion, but they often affect the absorption performance of absorbents. Therefore,

Table 4. Absorption performance of NE-1 and MEA system.

| System | Absorption temperature/°C | Saturation time/min | CO ₂ loading/mol·kg ⁻¹ |
|------------|---------------------------|---------------------|--|
| 45% NE-1 | 40 | 136 | 3.51 |
| 45% NE-1a1 | | 151 | 3.71 |
| 45% NE-1b1 | | 176 | 3.62 |
| 45% NE-1c1 | | 231 | 3.73 |
| 30% MEA | | 180 | 2.83 |

the influence of three typical corrosion inhibitors (carbamide, methionine, and malondiamine acetic acid) on the CO₂ absorption performance of NE-1 was investigated. By monitoring the absorption rate, as shown in Fig. 9, 45% NE-1a1 system still maintains a high absorption rate under high CO₂ loading (50%–60% of the equilibrium loading). Although the 45% NE-1c1 system has the highest absorption capacity, it still takes 100 min to reach absorption equilibrium after reaching 95% saturation absorption capacity.

The CO₂ loading of the NE-1 system with corrosion inhibitor has significantly increased, but the time for absorption saturation is also longer. Among the three absorption systems with added corrosion inhibitors, 45% NE-1a1 exhibited high CO₂ loading (3.71 mol/kg) and the shortest absorption saturation time (151 min). Compared with commercial 30% MEA, 45% NE-1a1 has a 32% increase in CO₂ absorption capacity and 16% reduction in saturation time (Table 4).

Furthermore, the cycling stability of NE-1 absorbent was investigated. A 45% concentration of NE-1 decarbonization agent was selected to absorb CO₂ at 40 °C and regenerate at 100 °C. The loading amount

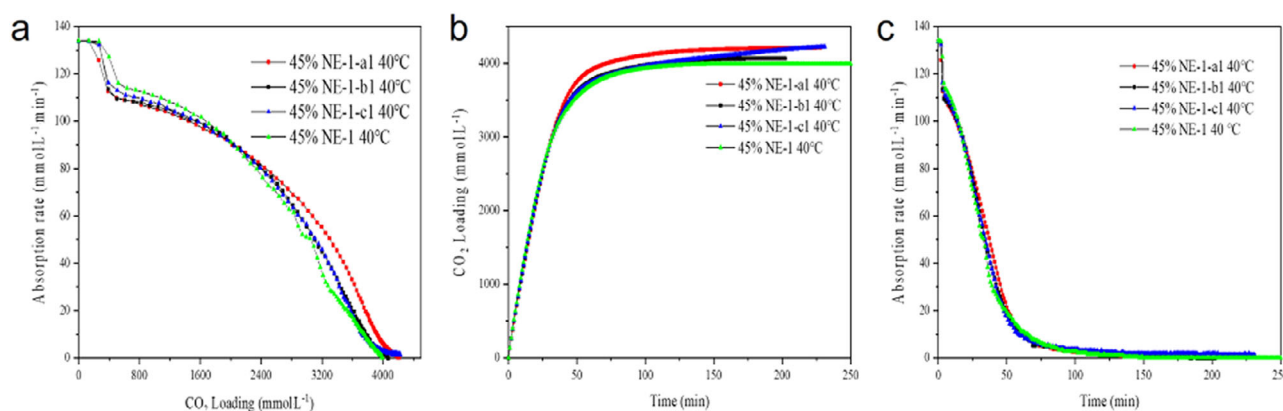
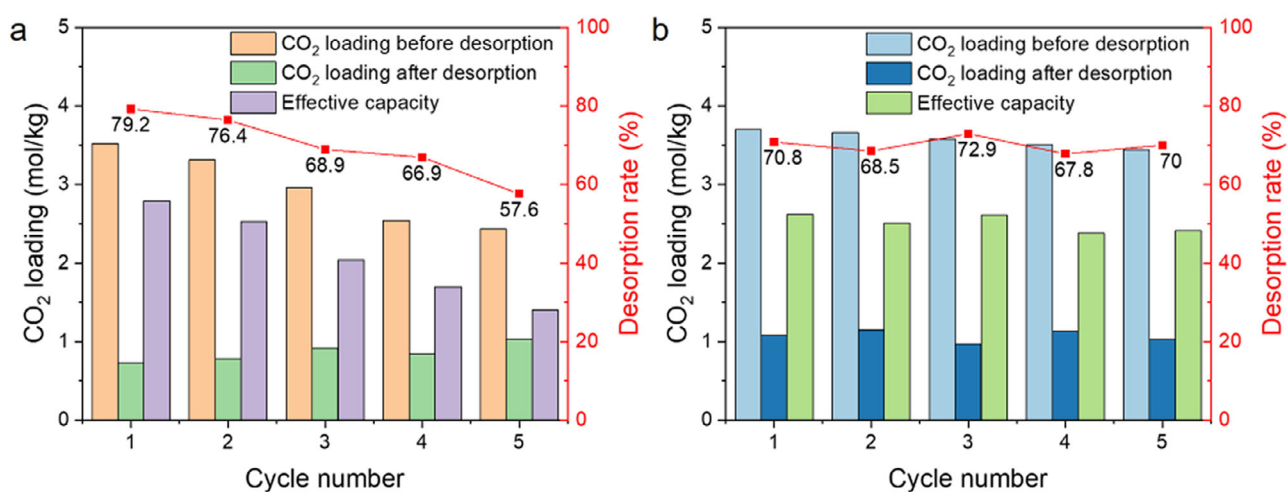


Figure 9. Absorption rate of 45% NE-1 corrosion inhibitor system.

Table 5. Absorption/desorption cycle performance of 45% NE-1.

| Cycle number | Saturation time/min | CO ₂ loading/mol·kg ⁻¹ | | Effective capacity /mol·kg ⁻¹ | Desorption rate /% |
|--------------|---------------------|--|------------------|--|--------------------|
| | | Before desorption | After desorption | | |
| 1 | 135 | 3.52 | 0.73 | 2.79 | 79.2 |
| 2 | 140 | 3.31 | 0.78 | 2.53 | 76.4 |
| 3 | 142 | 2.96 | 0.92 | 2.04 | 68.9 |
| 4 | 145 | 2.54 | 0.84 | 1.70 | 66.9 |
| 5 | 146 | 2.43 | 1.03 | 1.40 | 57.6 |

**Figure 10. Cycle stability performance of NE-1 absorbent (a) 45% NE-1; (b) 45% NE-1a1.**

before and after desorption was measured by the titration method. The test results are shown in Table 5. After five cycles, the cycling capacity of the 45% NE-1 system descended to 2.43 mol/kg, the effective desorption capacity was only 1.40 mol/kg, and the desorption rate decreased from initial 79.2% to 57.6% (Fig. 10a). Since part of CO₂ exists as a thermally stable salt and cannot be completely regenerated at 100 °C, the absorption solution still contains about 0.8–1.0 mol/kg of CO₂ after desorption. As the cycle number increases, the content of thermal stability salts slightly rise, which may be due to the measured CO₂ concentration being too high caused by purge N₂ carrying water away from the solution. The gradual decrease in CO₂ saturation absorption capacity indicates that NE-1 may undergo decomposition during thermal regeneration, leading to stability issues.

However, for the sample with the added corrosion inhibitor carbamide (NE-1a1), the CO₂ effective desorption capacity remained 2.50 mol/kg and the CO₂

desorption efficiency can be maintained at 70% during five absorption/desorption cycles (Fig. 10b), reflecting the promoting effect of carbamide on the stability of NE-1 absorbent.

Finally, we investigated the effect of corrosion inhibitors on the thermal stability of NE-1. The GC-MS analysis results of NE-1 samples with and without corrosion inhibitors added are shown in Table 6. After 50 hr of thermal treatment in an anaerobic atmosphere at 120 °C, a small amount of pyrazine (0.55%) appeared in the 45% NE-1 sample, while the ratio of 2-hydroxyethyl ethylamine (C₄H₁₁NO) and 1-piperazine ethylamine (C₆H₁₅N₃) changed significantly. This indicates that NE-1 is prone to decomposition during high-temperature regeneration. However, the NE-1 sample with added corrosion inhibitor did not detect pyrazine after thermal treatment. Especially for the 45% NE-1a1 sample, the content of 2-hydroxyethyl ethylamine and 1-piperazine ethylamine in the solution remained unchanged before

Table 6. GC-MS data of 45% NE-1 and corrosion inhibitor before and after thermal degradation.

| Sample | Number | Time (min) | Chemical formula | Molar mass | CAS | Relative peak area (%) | |
|------------|--------|------------|---|------------|----------|----------------------------|---------------------------|
| | | | | | | Before thermal degradation | after thermal degradation |
| 45% NE-1 | 1 | 3.43 | C ₄ H ₄ N ₂ | 80 | 290-37-9 | - | 0.55 |
| | 2 | 4.58 | C ₄ H ₁₁ NO | 89 | 110-73-6 | 57.03 | 27.07 |
| | 3 | 11.7 | C ₆ H ₁₅ N ₃ | 129 | 140-31-8 | 42.97 | 72.38 |
| 45% NE-1a1 | 1 | 4.58 | C ₄ H ₁₁ NO | 89 | 110-73-6 | 63.21 | 59.35 |
| | 2 | 11.7 | C ₆ H ₁₅ N ₃ | 129 | 140-31-8 | 36.79 | 40.65 |
| 45% NE-1b1 | 1 | 4.58 | C ₄ H ₁₁ NO | 89 | 110-73-6 | 52.51 | 34.87 |
| | 2 | 11.7 | C ₆ H ₁₅ N ₃ | 129 | 140-31-8 | 47.49 | 65.13 |
| 45% NE-1c1 | 1 | 4.58 | C ₄ H ₁₁ NO | 89 | 110-73-6 | 15.95 | 46.09 |
| | 2 | 11.7 | C ₆ H ₁₅ N ₃ | 129 | 140-31-8 | 84.05 | 53.91 |

and after thermal degradation, which reflects the key role of carbamide as a corrosion inhibitor in inhibiting the thermal decomposition of NE-1.

Conclusion

This paper systematically investigated the physicochemical properties, CO₂ absorption and desorption performance, and stability of the NE-1 absorbent. The optimal operating conditions for NE-1 absorption of CO₂ were determined to be 45% NE-1 concentration, absorption at 40 °C, and regeneration at 100 °C. Compared to commercial 30% MEA, NE-1 has significant advantages in terms of absorption capacity, absorption rate, and desorption efficiency. The effects of the addition of three inhibitors on the solvent absorption and thermal degradation properties were determined. The NE-1 system may attain an effective CO₂ capacity of 2.5 mol/kg and a 70% desorption rate in five cycles by adding carbamide as a corrosion inhibitor to alleviate the thermal degradation of NE-1 in regeneration process. The research results have guiding significance for the development of efficient and stable industrial absorbent and supporting absorption/desorption process.

Acknowledgements

This work was financially supported by the Science and Technology Major Project of CNPC (No. 2021ZZ01), the Scientific Research and Technological Development Project of PetroChina Southwest Oil & Gasfield Company (No. 20220306-09), the Science and

Technology Project of PetroChina Oil&Gas and New Energy Branch (No. 2023YQX105).

References

1. Abdelkareem MA, Elsaid K, Wilberforce T, Kamil M, Sayed ET, Olabi A. Environmental aspects of fuel cells: a review. *Sci Total Environ.* 2021;752:141803.
2. Figueres C, Le Quéré C, Mahindra A, Bäte O, Whiteman G, Peters G, et al. Emissions are still rising: ramp up the cuts. *Nature.* 2018;564(7734):27–30.
3. Dai HL, Su YN, Liu JZ, Gu D, Kuang L, Zou C. Thinking of China's energy development strategy under carbon neutrality goal. *Pet Sci Technol Forum.* 2022;41(01):1–8.
4. Liu ZG. Research status and development trend of CO₂ capture technology. *Chem Eng Oil Gas.* 2022;51(4):24–32.
5. Matter JM, Stute M, Snæbjörnsdóttir SÓ, Oelkers EH, Gislason SR, Aradóttir ES, et al. Rapid carbon mineralization for permanent disposal of anthropogenic carbon dioxide emissions. *Science.* 2016;352(6291):1312–14.
6. Feng B, Du M, Dennis TJ, Anthony K, Perumal MJ. Reduction of energy requirement of CO₂ desorption by adding acid into CO₂-loaded solvent. *Energy Fuels.* 2010;24(1):213–19.
7. Idem R, Wilson M, Tontiwachwuthikul P, Chakma A, Veawab A, Aroonwilas A, et al. Pilot plant studies of the CO₂ capture performance of aqueous MEA and mixed MEA/MDEA solvents at the University of Regina CO₂ capture technology development plant and the boundary dam CO₂ capture demonstration plant. *Ind Eng Chem Res.* 2006;45 (8):2414–20.
8. Chen SJ, Zhu M, Fu Y, Huang YX, Tao ZC, Li WL. Using 13X, LiX, and LiPdAgX zeolites for CO₂ capture from post-combustion flue gas. *Appl Energy.* 2017;191:87–98.
9. Yue H, Zhao Y, Zhao Li, Lv J, Wang S, Gong J, et al. Hydrogenation of dimethyl oxalate to ethylene glycol on a Cu/SiO₂/cordierite monolithic catalyst: enhanced internal mass transfer and stability. *AIChE J.* 2012;58(9):2798–809.
10. Kittel J, Gonzalez S. Corrosion in CO₂ post-combustion capture with alkanolamines - a review. *Oil Gas Sci Technol-Revue D'IFP Energies Nouvelles.* 2014;69(5):915–29.

11. Kittel J, Fleury E, Vuillemin B, Gonzalez S, Ropital F, Oltra R. Corrosion in alkanolamine used for acid gas removal: from natural gas processing to CO₂ capture. *Mater Corros-Werkst Korros*. 2012;63(3):223–30.
12. Hasib-ur-Rahman M, Sijaj M, Larachi F. Ionic liquids for CO₂ capture-development and progress. *Chem Eng Process-Process Intensif*. 2010;49(4):313–22.
13. Zhang X, Zhang X, Dong H, Zhao Z, Zhang S, Huang Y. Carbon capture with ionic liquids: overview and progress. *Energy Environ Sci*. 2012;5(5):6668–81.
14. Zhu K, Lu H, Liu C, Wu K, Jiang W, Cheng J, et al. Investigation on the phase-change absorbent system MEA plus solvent A (SA) + H₂O used for the CO₂ capture from flue gas. *Ind Eng Chem Res*. 2019;58(9):3811–21.
15. Zhang S, Shen Y, Wang L, Chen J, Lu Y. Phase change solvents for post-combustion CO₂ capture: principle, advances, and challenges. *Appl Energy*. 2019;239:876–97.
16. Liang B, Shen KJ, Li GH, Tang SY, Zhong S. Study on the anion migration in the CO₂ mineralization process coupled with organic amine extraction. *Chem Eng Oil Gas*. 2022;51(5):60–64.
17. Machida H, Ando R, Esaki T, Yamaguchi T, Horizoe H, Kishimoto A, et al. Low temperature swing process for CO₂ absorption-desorption using phase separation CO₂ capture solvent. *Int J Greenhouse Gas Control*. 2018;75:1–7.
18. Barbarossa V, Barzagli F, Mani F, Lai S, Stoppioni P, Vanga G. Efficient CO₂ capture by non-aqueous 2-amino-2-methyl-1-propanol (AMP) and low temperature solvent regeneration. *RSC Adv*. 2013;3(30):12349–55.
19. Barzagli F, Mani F, Peruzzini M. Efficient CO₂ absorption and low temperature desorption with non-aqueous solvents based on 2-amino-2-methyl-1-propanol (AMP). *Int J Greenhouse Gas Control*. 2013;16:217–23.
20. Fan ML, Hua YH, Su QB. Design of amine decarbonization process for high CO₂ content natural gas. *Chem Eng Oil Gas*. 2021;50(2):35–41.
21. Li J, You C, Chen L, Ye Y, Qi Z, Sundmacher K. Dynamics of CO₂ absorption and desorption processes in alkanolamine with cosolvent polyethylene glycol. *Ind Eng Chem Res*. 2012;51(37):12081–88.



Chenzhi Huang

Chenzhi Huang is an engineer at the Research Institute of Natural Gas Technology, PetroChina Southwest Oil & Gasfield Company. His research topics include petroleum, natural gas, new energy, and CCUS.



Yongda Cao

Yongda Cao is an engineer at the Research Institute of Natural Gas Technology, PetroChina Southwest Oil & Gasfield Company. Her research focuses on CCUS and distributed photovoltaic.



Yaxin Li

Yaxin Li is an engineer at the Research Institute of Natural Gas Technology, PetroChina Southwest Oil & Gasfield Company, mainly working in the direction of CCUS.



Qi Li

Qi Li is a senior engineer at PetroChina Southwest Oil & Gasfield Company. Her research topics include wind and solar power generation, hydrogen energy, CCUS, and geothermal energy.



Qiang Liu

Qiang Liu is a senior engineer at the New Energy Division, PetroChina Southwest Oil & Gasfield Company. Her research topics include hydrogen energy, CCUS, and photovoltaic power generation.



Lin Xia

Lin Xia is an engineer at the Natural Gas Purification Plant of PetroChina Southwest Oil & Gasfield Company. His research topics include petroleum, natural gas, new energy, and CCUS, and residual pressure power generation.



Xiujun Peng

Xiujun Peng is a senior engineer at Research Institute of Natural Gas Technology, PetroChina Southwest Oil & Gasfield Company. His research topics include natural gas purification and carbon capture.



Hairong Yue

Hairong Yue received his Ph.D. degree from Tianjin University (China) in 2012. He has been a Professor at School of Chemical Engineering, Sichuan University, China since 2018. His research interests lie in the carbon capture, sequestration and chemical conversion, catalytic synthesis of ethylene glycol/ethanol from syngas, production and storage of hydrogen energy.